Cerebral Hemodynamics in CADASIL Before and After Acetazolamide Challenge Assessed With MRI Bolus Tracking

H. Chabriat, MD, PhD; S. Pappata, MD; L. Ostergaard, PhD; C.A. Clark, PhD;
M. Pachot-Clouard, PhD; K. Vahedi, MD; A. Jobert, BSc; D. Le Bihan, MD, PhD; M.G. Bousser, MD

Background—White matter lesions in cerebral autosomal dominant arteriopathy with subcortical infarcts and leukoencephalopathy (CADASIL) are underlaid by severe ultrastructural changes of the arteriolar wall. Although chronic ischemia is presumed to cause the tissue lesions, the pattern of perfusion abnormalities and hemodynamic reserve in CADASIL, particularly within the white matter, remains unknown.

Methods—We used the MRI bolus tracking method in 15 symptomatic patients with CADASIL (5 with dementia) and 10 age-matched control subjects before and 20 minutes after the intravenous injection of acetazolamide (ACZ, 17 mg/kg). Cerebral blood flow (CBF), blood volume (CBV), and mean transit time (MTT) were calculated both in the cortex and in the white matter according to the singular value decomposition technique. Perfusion parameters were obtained in regions of hyperintensities and within the normal-appearing white matter as observed on T2-weighted images. Analysis was performed with both absolute and relative (region/whole brain) values.

Results—A significant reduction in absolute and relative CBF and CBV was found within areas of T2 hyperintensities in white matter in the absence of significant variations of MTT. This reduction was more severe in demented than in nondemented patients. No significant change in absolute CBF and CBV values was observed in the cortex of patients with CADASIL. A decrease in relative CBF and CBV values was detected in the occipital cortex. After ACZ administration, CBF and CBV increased significantly in both the cortex and white matter of affected subjects, but the increase in absolute CBF was lower within areas of increased signal on T2-weighted images in patients than in the white matter of control subjects.

Conclusions—In CADASIL, both basal perfusion and hemodynamic reserve are decreased in areas of T2 hyperintensities in the white matter. This hypoperfusion appears to be related to the clinical severity. The significant effect of ACZ on CBF and CBV suggests that cerebral perfusion might be increased using pharmacological vasodilation in CADASIL. (*Stroke*. 2000;31:1904-1912.)

Key Words: acetazolamide ■ CADASIL ■ magnetic resonance imaging ■ leukoaraiosis ■ perfusion

Cerebral autosomal dominant arteriopathy with subcortical infarcts and leukoencephalopathy (CADASIL) is a small-artery disease secondary to mutations of *Notch* 3 gene.[1,2] The clinical presentation includes migraine with aura, mood disorders, subcortical ischemic strokes, and dementia.[3] One hallmark of CADASIL is the presence of widespread increased signal intensities in the white matter on T2-weighted MRIs.[4,5] These white matter signal abnormalities (WMAs) are not only constant in symptomatic carriers of the mutated gene but also frequent in asymptomatic ones.[2,3] They are often associated with typical white matter or basal ganglia infarcts.[4,6,7] Pathological data reveal a severe white matter rarefaction associated with lacunar infarcts.[8] We recently showed that the severity of white matter microstructural changes measured in vivo with diffusion tensor imaging is related to the clinical severity in CADASIL.[9]
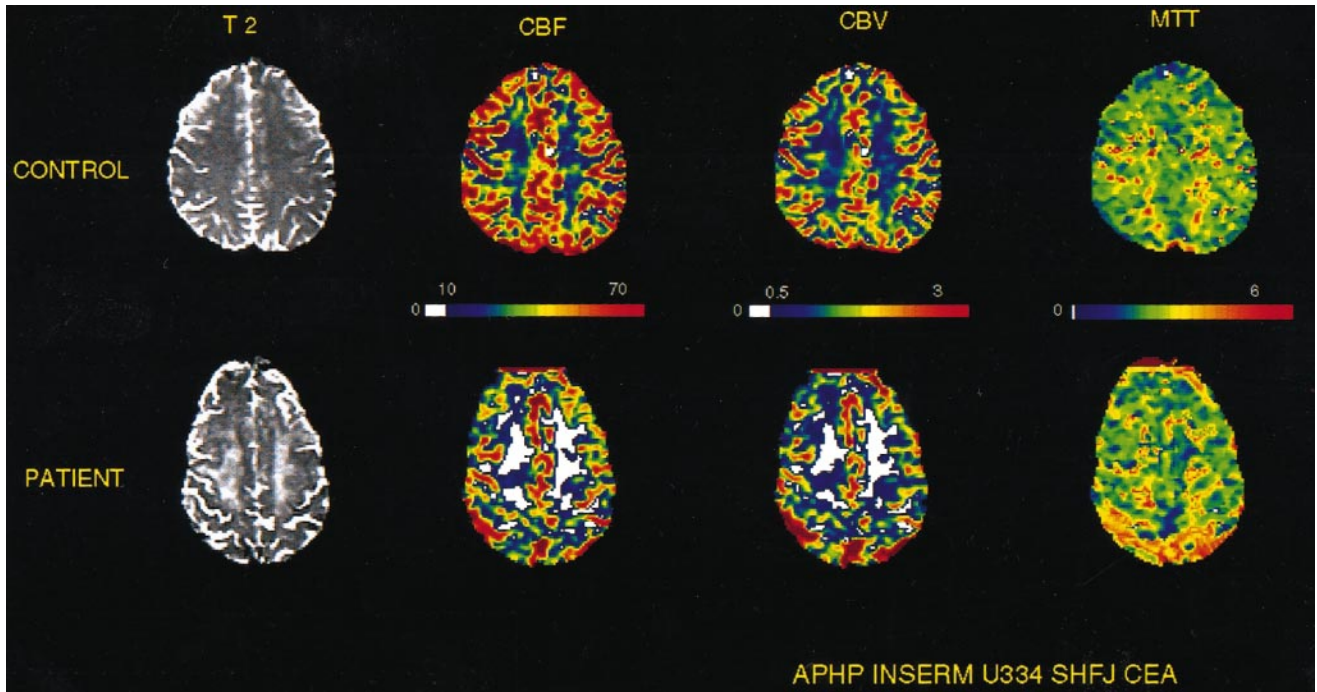
White matter lesions in CADASIL are underlaid by characteristic ultrastructural modifications of the arteriolar wall.[8] An electron-dense granular material of undetermined origin is present within the media of perforating cerebral arteries,[8,10] adjacent to degenerated smooth muscle cells. The physiopathological link between these structural vascular changes and the white matter lesions has not been investigated so far. The only 2 neuroimaging studies of perfusion in patients with CADASIL were focused on cortical blood flow changes.[11,12]

MR images obtained in 1 control subject (top row) and 1 patient with CADASIL. CBF of <10 mL $\cdot$ 100 mL^{-1} $\cdot$ min^{-1} and CBV of <0.5 mL $\cdot$ 100 mL^{-1} are shown in white. Note that the pattern of hypoperfusion in white matter is close to the pattern of increased signal as seen on T2-weighted images. No significant change of MTT was observed in the patient with CADASIL.

To address this issue, we chose to study cerebral perfusion before and after acetazolamide (ACZ) challenge by using the MRI bolus tracking method. Recently, the "singular value decomposition" technique was proposed to deconvolve the arterial input function and tissue signal changes after gadolinium injection for the quantification of cerebral blood flow (CBF), cerebral blood volume (CBV), and mean transit time (MTT) with MRI.[13,14] This quantitative method has been validated with parallel PET studies.[15,16] The corresponding quantification is reported to be sensitive to blood flow changes with CO_2.[15] Such MRI methods provide both the advantage of easy registration of perfusion images with T1- or T2-weighted images and the advantage of high spatial resolution, which is crucial for an evaluation of hemodynamics in various areas of white matter.

Subjects and Methods

Subjects

Fifteen patients with CADASIL were selected (mean age 58 ± 7 years). All had deleterious mutations of *Notch* 3 gene on chromosome 19.[17] The patients underwent a detailed neurological examination that preceded the MRI examination and included a brief evaluation of the cognitive deficit with the Mini-Mental Status Examination (MMSE)[18] and the degree of handicap with the Rankin Score.[19] None of them presented with carotid or vertebral stenosis based on the results of previous duplex scanning examination or magnetic resonance angiography.

All patients were symptomatic. Eight had a previous history of recurrent attacks of migraine with aura, and 11 had a history of transient ischemic attacks or completed strokes. Six patients presented with focal neurological deficits at the time of MRI examination. Five of them satisfied the DSM III criteria for dementia, had an MMSE score of <25,[20] and had a Rankin Score of >2. Only 1 patient was severely demented and bedridden. In nondemented

subjects, handicap was absent or slight except in 1 patient who had a Rankin Score of 3.

Ten healthy volunteers >40 years old (mean age 53 ± 8 years) were used as control subjects. They all fulfilled the following criteria: (1) no familial vascular disorder, (2) no history of neurological disorder, (3) normal neurological and general examinations, (4) MMSE score of >28, and (5) normal T1- and T2-weighted MRIs.

Informed consent was obtained from each subject or from the closer relative if he or she was too severely disabled to provide written consent. This study was approved by an independent ethical committee (CCPPRB Bicêtre 9724).

MRI

Imaging Protocol

Studies were performed with a 1.5-T Signa Horizon Echospeed MRI system (Signa General Electric Medical Systems). Head movements were reduced with pillows placed on both sides of the head, which was also maintained with a fixed strap positioned around the forehead.

Perfusion images were obtained after the acquisition of T1- and T2-weighted images . T1-weighted images were acquired in the axial plane with a spoiled gradient echo sequence (124 slices 1.2 mm thick, TR 10.3 ms, TE 2.1 ms, TI 600 ms, and 24$\times$24-cm field of view). T2-weighted images were obtained at 4 echo times (40, 80, 120, and 160 ms) with a multiecho spin-echo sequence with TR of 3500 ms in the axial plane (20 slices 5 mm thick) and a 24$\times$24-cm field of view.

For perfusion studies, asymmetric spin-echo (TR 1600 ms, TE 80 ms, asymmetry delay 20 ms) echo-planar imaging (EPI) was performed starting 30 seconds before injection of the tracer. This sequence was chosen to detect sufficient signal variations with a single dose of 0.1 mmol/kg gadolinium within the affected white matter of the patients.[21] It was also preferred to the gradient echo EPI sequence, which is generally assumed to be more sensitive to signal changes within large vessels.[21,22] A 128$\times$128 acquisition matrix was used with a 24$\times$24-cm field of view, leading to an in-plane resolution of 1.875×1.875 mm^2. Seven slices, 5 mm thick, were acquired every 1.6 seconds from the cerebellar level up to the

TABLE 1. Averaged CBF, CBV, and MTT Values in All Regions Before and After ACZ in Patients and Control Subjects

Region	CBF, mL · 100 mL⁻¹ · min⁻¹			CBV, mL · 100 mL⁻¹		
	Patients	Control Subjects	Group/ACZ/Interaction P	Patients	Controls	Group/ACZ/Interaction P
Cortex frontal	49.6±22.3	50.8±21.5	0.7/0.0001/0.7	2.06±0.74	2.38±0.70	0.3/0.0001/0.9
	80.1±38.1	85.1±41.1		3.22±1.17	3.57±1.23	
Cortex parietal	51.7±23.5	54.0±26.0	0.7/0.0001/0.7	2.29±0.82	2.59±0.86	0.3/0.0001/0.7
	84.4±36.4	90.1±48.9		3.34±0.96	3.75±1.39	
Cortex occipital	58.4±28.4	68.2±30.5	0.3/0.0001/0.4	2.81±1.17	3.38±1.18	0.1/0.0001/0.6
	94.2±44.0	113.8±58.8		3.90±1.31	4.69±1.70	
Basa lganglia	51.7±31.2	52.1±23.1	0.7/0.0001/0.3	2.15±1.02	2.50±0.86	0.4/0.0001/0.8
	72.9±41.0	82.6±51.3		2.92±1.22	3.22±1.55	
C semiovale (whole)	**17.3±11.5**	...	0.05/0.0001/0.1	**0.78±0.39**	...	0.001/0.0001/0.06
	23.3±12.0	...		1.02±0.44	...	
WMA	**13.2±6.5**	22.7±8.6	0.007/0.0001/0.04	**0.63±0.31**	1.24±0.38	0.0023/0.0001/0.3
	19.7±9.9	35.3±13.8		**0.95±0.51**	1.72±0.63	
NAWM	23.2±9.0	...	0.5/0.0007/0.6	1.10±0.38	...	0.2/0.003/0.6
	33.0±14.1	...		1.44±0.48	...	

Bold/underlined values are statistically different from control values.

centrum semiovale, with an interslice gap of 5 mm. The slice levels were chosen based on previously acquired T2-weighted images so the second or third lowest slices included the M1 portion of middle cerebral artery (MCA) and 1 of the highest planes (sixth or seventh plane) crossed the centrum semiovale of both right and left hemispheres above the ventricles. Bolus injection was performed manually by the same examiner (HC) at a rate of 5 to 10 mL/s in an antecubital vein and was followed by the injection of 50 mL of saline flush. A dose of 0.1 mmol/kg gadoteric acid (DOTAREM) was used before and 20 minutes after the intravenous injection of 17 mg/kg ACZ[23] (DIAMOX). A total of 73 images were acquired for each slice. The duration of each perfusion experiment was 1 minute 56 seconds.

Quantification of Perfusion Parameters

The analysis was performed blinded to the subjects' clinical condition. The quantification was based on susceptibility contrast arising from compartmentalization of the paramagnetic agents[24] and pre-sumed a linear relationship between paramagnetic tracer concentration and the change of transverse relaxation rate, ΔR_2.[25] ΔR_2 was consequently used to obtain tissue and arterial tracer time concentration curves C(t) according to the equation

$$C(t) \propto \Delta R_2(t) = -\log[S(t)/S(0)]/TE$$

where S(0) and S(t) are the signal intensities at baseline and time t, respectively.[14]

We performed repeated T1-weighted MRI every 10 minutes for 40 minutes in 2 patients and 60 minutes in a third patient to verify the absence of signal enhancement after a dose of 0.1 mmol/kg gadoteric acid. No signal enhancement was detected in 5 regions of interest (ROIs) (surface 1.5 cm²) positioned in the normal (2 ROIs) or abnormal (3 ROIs) white matter as seen on T2-weighted images. This indicated that there was no disruption of the blood-brain barrier in normal-appearing white matter (NAWM) and lesions in our patients. This was a necessary condition for the quantification of cerebral perfusion with dynamic susceptibility enhanced MRI.

TABLE 2. Mean Relative CBF, CBV, and MTT Values in Patients and Control Subjects

Region	relCBF			relCBV		
	Patients	Control Subjects	Group/ACZ/Interaction P	Patients	Control Subjects	Group/ACZ/Interaction P
Cortex frontal	0.96±0.10	0.94±0.12	0.6/0.6/0.8	0.90±0.10	0.92±0.14	0.3/0.0001/0.5
	0.97±0.14	0.95±0.06		0.97±0.14	0.96±0.06	
Cortex parietal	0.99±0.07	0.98±0.05	0.2/0.07/0.2	0.99±0.09	0.98±0.06	0.3/0.0001/0.6
	1.03±0.05	0.99±0.03		1.02±0.07	1.00±0.03	
Cortex occipital	**1.10±0.10**	1.25±0.04	0.0001/0.1/0.4	**1.18±0.08**	1.27±0.08	0.005/0.1/0.7
	1.13±0.09	1.26±0.06		**1.17±0.08**	1.25±0.03	
Basal ganglia	0.99±0.28	0.94±0.33	0.9/0.3/0.2	0.94±0.26	1.03±0.23	0.3/0.1/0.8
	0.90±0.28	0.95±0.13		0.89±0.27	1.00±0.18	
C semiovale (whole)	0.34±0.10	...	0.02/0.1/0.3	**0.35±0.10**	...	0.006/0.06/0.1
	0.30±0.11	...		**0.32±0.11**	...	
WMA	**0.26±0.15**	0.43±0.06	0.008/0.4/0.5	**0.28±0.15**	0.47±0.07	0.005/0.6/0.4
	0.26±0.12	0.41±0.08		**0.29±0.15**	0.46±0.06	
NAWM	0.46±0.19	...	0.6/0.4/0.9	0.48±0.16	...	0.9/0.5/0.9
	0.44±0.17	...		0.46±0.16	...	

Bold/underlined values are statistically different from control values.

TABLE 1.   Continued

	MTT, s	
Patients	Control Subjects	Group/ACZ/Interaction P
2.67±0.64	2.99±0.63	0.5/0.5/0.4
2.70±0.94	2.76±1.08	
2.84±0.69	3.05±0.52	0.6/0.09/0.6
2.66±0.92	2.73±0.99	
3.08±0.80	3.12±0.57	0.9/0.004/0.7
2.75±0.84	2.70±0.99	
2.71±0.72	2.92±0.56	0.5/0.9/0.9
2.71±0.95	2.88±1.06	
2.99±0.76	...	0.3/0.2/0.5
2.87±0.93	...	
2.97±0.55	3.45±0.68	0.4/0.7/0.4
3.05±1.20	3.08±1.01	
2.95±0.66	...	0.3/0.4/0.4
2.90±1.08	...	

The arterial concentration was determined in each patient with 1 slice from pixels that contained the M1 portion of the MCA.[14] Five pixels, showing the largest and most narrow and early ΔR_2 value in close vicinity of the M1 portion of MCA, were used to obtain the arterial input function (AIF) for the first perfusion study in all subjects. This region was copied onto images obtained during the second bolus injection after ACZ injection, with the assumption that the head movements were insignificant between the first and second perfusion studies. In each case, we verified that the copied region determined a typical arterial curve (early and large signal decrease) on the second examination. The area under the arterial input function was carefully calculated to allow the quantification of absolute CBF. To avoid bias due to tracer recirculation at the end of the first pass, we tested the stability of determining the area through numerical integration of the AIF and correction for recirculation by (1) fitting the down slope of the AIF to a straight line and by (2) fitting the AIF to a γ- variate function. By visual inspection, we found that the linear fitting would better fit the end of the slope than a γ-variate function in most of our subjects, particularly after ACZ administration, which accelerates the occurrence of recirculation. Thereafter, the integrated

TABLE 2.   Continued

	relMTT	
Patients	Control Subjects	Group/ACZ/Interaction P
0.93±0.06	0.95±0.04	0.1/0.0001/0.008
1.42±0.13	1.30±0.11	
0.98±0.05	0.98±0.03	0.04/0.0001/0.01
1.39±0.08	1.30±0.09	
1.07±0.08	1.00±0.05	0.0007/0.0001/0.01
1.46±0.12	1.28±0.09	
1.08±0.37	0.87±0.21	0.08/0.5/0.2
1.16±0.32	0.89±0.32	
1.05±0.11	...	0.2/0.06/0.7
1.11±0.17	...	
1.08±0.08	1.08±0.08	0.8/0.1/0.7
1.20±0.34	1.15±0.10	
1.04±0.14	...	0.6/0.06/0.9
1.12±0.19	...	

area of AIF was calculated and normalized, in each measurement, to the injected dose in mmol/kg for comparison within and among patients. At the present time, calibration factors to estimate CBF have been reported only for spin-echo EPI.[15] To obtain the CBF value for the asymmetrical spin-echo sequence with the singular value decomposition technique, a common conversion factor[13] was determined between MRI flow units and absolute flow in mL · 100 mL^{-1} · min^{-1}, so the mean CBF in the white matter of the 5 control subjects first recruited in our center was 23 mL · 100 mL^{-1} · min^{-1}.[26] The CBV was calculated by integrating the area under the tissue concentration time curve during the first tracer passage. Deconvolution of tissue time curves by the arterial input function was performed after smoothing of raw images with a 3×3 uniform kernel. For deconvolution, the arterial curve obtained on 1 plane as detailed was used separately for each plane after correction for the delay between slices with Fourier interpolation.[27] In the absence of stenosis of large arteries in all subjects, we assume that delays in arrival time did not differ between patients and control subjects. The maximum of the deconvolved response curve was assumed to be proportional to CBF.[13] The MTT used in our analysis was calculated as the ratio of CBV to CBF in each ROI.

Regions of Interest

In each subject, circular ROIs (surface of each 0.5 cm^2) were defined on the first raw image (T2 weighted) of the perfusion sequence with reference to the Talairach-Tournoux stereotaxic atlas.[28] ROIs were carefully positioned along the cortical rim to exclude contamination from large vessels such as MCA or large venous sinuses[29] and EPI susceptibility artifacts in temporal and mediofrontal cortical regions.[30]

In the white matter, a set of circular ROIs was placed similarly in all subjects on 1 plane that passed through the centrum semiovale. First, a global "centrum semiovale" region was generated (total surface 13 cm^2) that included ROIs independently of the presence or absence of T2 hyperintensities. Second, 2 smaller regions (surface 2 cm^2) were obtained: 1 in the NAWM and another within T2 signal abnormalities (WMA). Circular ROIs were positioned in the cerebral cortex, thalamus, and basal ganglia (putamen and caudate) over the different planes and grouped into various anatomic regions.

Averaged CBF, CBV, and MTT values of each structure were then calculated for both hemispheres. To reduce the interindividual variability, regional cortical and white matter CBF, CBV, and MTT values were also normalized for the global corresponding value in each subject and expressed as relative values: relCBF, relCBV, and relMTT.

Statistical Analysis

For each region, a 2-way repeated measures ANOVA was performed with group (patients and control subjects) and ACZ effect (measures before and after ACZ) as factors on absolute and relative CBF, CBV, and MTT values. To compare the perfusion parameters between demented and nondemented patients, a separate 2-way repeated measures ANOVA was performed with group (demented and non-demented) and ACZ effect as factors on absolute and relative CBF and CBV values obtained in patients.

The Fisher's test of protected least significant difference was used for post hoc analysis of multiple comparisons only if the group difference, ACZ effect, or interaction between group and ACZ effect was significant.

Values of $P<0.05$ were considered statistically significant. Data are presented as mean±SD. The statistical analysis was performed with GB-STAT Version 6.5 PPC software (Dynamic Microsystem Inc).

Results

Averaged CBF, CBV, and MTT values calculated in all regions, before and after ACZ administration, in both patients and control subjects are presented in Table 1. In control subjects, at the cortical level, mean coefficient of variation values of baseline CBF, CBV, and MTT varied from 42% to

48%, 29% to 35%, and 17% to 19%, respectively. The ACZ challenge induced a significant increase of global CBF (baseline 55.3 ± 27 mL $\cdot$ 100 mL^{-1} $\cdot$ min^{-1}, after ACZ 90.1 ± 46.9 mL $\cdot$ 100 mL^{-1} $\cdot$ min^{-1}; $+63\%$, $P<0.0001$) and CBV (baseline 2.69 ± 0.96 mL $\cdot$ 100 mL^{-1}, after ACZ 3.75 ± 1.40 mL $\cdot$ 100 mL^{-1}; $+39\%$, $P<0.0001$) and a significant decrease of global MTT (baseline 3.14 ± 0.61 seconds, after ACZ 2.66 ± 0.95 seconds; -15%, $P=0.03$) in control subjects. The increase in CBF and CBV was significant in all regions. The decrease of MTT was significant only in the occipital cortex.

Comparison of Absolute Data Between Patients and Control Subjects

ANOVA showed a significant group effect on CBF and CBV measured in global centrum semiovale and WMA regions but not in the cerebral cortex (Figure; Table 1). The group$\times$ACZ interaction was significant only for CBF in WMA.

Both CBF and CBV were reduced in patients with CADA-SIL in the global centrum semiovale and WMA. In the global centrum semiovale, post hoc analysis showed that the group difference was significant only after ACZ administration for CBF and both before and after ACZ for CBV. In WMA, both pre- and post-ACZ CBF and CBV values were lower in patients than in control subjects. Only a trend for reduction in CBV was observed in cortical regions of patients.

The effect of ACZ challenge on CBF, CBV, and MTT did not differ between patients and control subjects in all regions except WMA. In this area, the absolute CBF increase after ACZ ($+6.6\pm6.8$ mL $\cdot$ 100 mL^{-1} $\cdot$ min^{-1}) was significantly lower than that observed in the white matter of control subjects ($+12.8\pm4.9$ mL $\cdot$ 100 mL^{-1} $\cdot$ min^{-1}; $P=0.02$). The difference between the CBV increase observed in patients ($+0.32\pm0.31$ mL $\cdot$ 100 mL^{-1}) and control subjects ($+0.48\pm0.36$ mL $\cdot$ 100 mL^{-1}) in the same region did not reach statistical significance.

Comparison of Relative Data Between Patients and Control Subjects

Mean relCBF, relCBV, and relMTT values in patients and control subjects are presented in Table 2. ANOVA showed a significant group effect on relCBF and relCBV measured in the centrum semiovale, WMA, and occipital cortex. There also was a significant group effect on relMTT measured in the parietal and occipital cortex. The group$\times$ACZ interaction was significant for relMTT in the frontal, parietal, and occipital cortex.

Before and after ACZ administration, both relCBF and relCBV were lower in patients with CADASIL than in control subjects in the centrum semiovale, in WMA, and in the occipital cortex. No significant difference of relMTT was detected in white matter. In the cortex, relMTT was higher in patients than in control subjects in the occipital region both before and after ACZ administration and in the parietal region only after ACZ. A significant increase in relMTT was detected in all cortical regions after ACZ administration. This effect was larger in the frontal, parietal, and occipital cortex in patients than in control subjects.

Comparison Between Demented and Nondemented Patients

ANOVA showed a significant difference between demented and nondemented patients only for absolute CBV and for both relCBF and relCBV in WMA (Table 3). Post hoc analysis revealed that baseline CBV and both baseline relCBF and baseline relCBV values in WMA were lower in demented than in nondemented patients. Also, we found a significant correlation between the MMSE score and 2 of these parameters measured in WMA: baseline absolute CBV ($\rho=0.61$, $P=0.02$) and relCBV ($\rho=0.64$, $P=0.01$). There was a trend between MMSE score and absolute or relCBF ($\rho=0.5$, $P=0.06$) in WMA.

Discussion

The averaged absolute CBF, CBV, and MTT values in our control subjects were close to those reported in previous MRI and PET studies.[26,31] In this series, the interindividual variability of normal CBF and CBV values obtained with an asymmetric spin-echo sequence and the singular value deconvolution technique was high (between 30% and 50%). However, a similar variability of absolute CBF and CBV data was reported in larger series of subjects with other MRI sequences and quantification methods.[31,32] This might be related to methodological limitations inherent to the MRI technique.[13] To calculate absolute values of CBF or CBV, the integrated area of the AIF was normalized to the injected dose of the tracer in each experiment. Although this method has been demonstrated to closely reflect the arterial concentrations of susceptibility contrast agents with spin-echo sequences, in the present study, the amplitude of signal changes for a similar bolus fraction can vary between individuals for different reasons. First, the location of pixels and slice position used to obtain the AIF can differ among individuals, leading to variations in the partial volume effect.[31] Second, in contrast to that observed with spin-echo sequences, the asymmetrical spin-echo signal changes due to the tracer passage is sensitive to local field inhomogeneities, which can also change between subjects in the region of MCA.[21] Third, our asymmetrical spin-echo sequence chosen to obtain the maximal sensitivity to microcirculatory blood volumes with a minimal dose of contrast agent is intermediate between the spin-echo and gradient-echo sequences.[21,22] This sequence remains strongly sensitive to signal variations within large vessels as shown by our CBF or CBV maps. Therefore, it is likely that there was different contamination of the tissue signal variations (presumed to be at the capillary level) by signal changes coming from large arteries or veins, particularly at the cortical level, despite our precautions to exclude the regions containing the largest vessels along the cortical rim.

We detected a major effect of ACZ on CBF and CBV in our healthy subjects. The mean 63% increase in CBF in healthy subjects is very close to that reported by other authors using similar MRI techniques.[29,31] Also, the ACZ effect on blood volume was comparable to that reported by Petrella et al[33] using a gradient-echo sequence and by Schreiber et al[31] with a dual fast low angle shot (FLASH) sequence. Interestingly, we also detected a global significant reduction in MTT after ACZ administration consistent with an increase in flow

TABLE 3. Absolute and Relative CBF and CBV Values for Demented and Nondemented Patients

Parameter	WMA			NAWM		
	Demented	Nondemented	Group/ACZ Effect *P*	Demented	Nondemented	Group/ACZ Effect *P*
Absolute values						
CBF baseline	8.4±8.0	15.79±11.6	0.1/0.0004	19.6±10.0	25.2±8.3	0.6/0.02
CBF after ACZ	15.7±11.6	22.02±8.76		33.8±19.5	32.6±11.6	
CBV baseline	**0.36±0.26**	**0.78±0.23**	0.04/0.003	0.97±0.54	1.17±0.26	0.1/0.04
CBV after ACZ	0.67±0.46	1.10±0.49		1.24±0.37	1.55±0.51	
Relative values						
CBF baseline	**0.14±0.09**	**0.33±0.14**	0.05/0.7	0.38±0.17	0.51±0.20	0.4/0.6
CBF after ACZ	0.19±0.09	0.29±0.11		0.42±0.23	0.45±0.15	
CBV baseline	**0.14±0.09**	**0.35±0.12**	0.02/0.4	0.39±0.18	0.53±0.15	0.1/0.6
CBV after ACZ	0.20±0.12	0.35±0.14		0.39±0.16	0.50±0.15	

CBF values are given as $mL \cdot 100 \ mL^{-1} \cdot min^{-1}$; CBV values, $mL \cdot 100 \ mL^{-1}$. Bold/underlined values are statistically different from control values.

velocities at the tissue level. Similar flow velocity changes have been previously reported in MCA and ophthalmic artery after ACZ challenge.[34,35] These results are in agreement with the prominent vasodilatory effect of the drug.[36] The exact mechanisms that underlie the vasodilatory effect of ACZ remain disputed and do not appear to be mediated by nitric oxide.[35] Overall, despite some limitations of our technique, the highly significant effect of ACZ in the present study supports the validity of the singular value decomposition technique to assess CBF, CBV, and MTT with MRI bolus tracking in the clinical setting.

We observed a significant decrease in absolute CBF values within the white matter of patients with CADASIL. The regional study indicates that hypoperfusion mainly concerns WMA. The pattern of maximal reduction of CBF was also very close to the topographical distribution of T2 signal abnormalities. Mean absolute CBF in WMA was 42% lower than that within the white matter of control subjects. These results are compatible with our previous PET findings in 2 patients with CADASIL.[11] The CBF decrease was also very similar to that previously reported in white matter of older patients with ischemic events or dementia in the presence of leukoaraiosis, presumably related to arteriosclerotic changes of perforating arteries.[37–39] In patients with CADASIL, we also observed a major reduction of CBV in WMA (≈50%). This decrease was parallel to the CBF decrease in the same area as reflected by the normal MTT. These results contrast with those of Turc et al,[40] who did not find significant CBV changes but only a reduction of CBF in white matter of patients with widespread leukoaraiosis of different origin. Nevertheless, both of their methods based on SPECT and radiolabeled blood cells and their population with heterogeneous clinical presentation greatly differ from ours. Our findings also differ with those of Yamaguchi et al,[41] who reported an increase of CBV in patients with WMA on T2-weighted images. However, their patients had a carotid occlusion, which might account for maximal vasodilation at the hemispheric level. In the present study, a trend for reduction of CBV was also detected in the NAWM, which suggests that the local reduction in baseline CBV related to

the small artery disease might play a crucial role in the white matter lesions in CADASIL.

Interestingly, we also found that the reduction of relative CBF or CBV in WMA was more severe in demented than in nondemented patients with CADASIL. Moreover, there was a significant correlation between the MMSE score and both absolute and relative CBV values in the same region. In our previous PET study of 2 patients with CADASIL with widespread WMA, we reported a 70% reduction in CBF in the white matter of the demented subject, whereas only a 46% CBF decrease was detected in the asymptomatic subject. Therefore, the severity of white matter hypoperfusion may be related to the clinical severity in CADASIL. A larger decrease of CBF in white matter has been related to dementia in leukoaraiosis associated with other types of microangiopathy.[37,42–44] Furthermore, Sabri et al[44] recently confirmed that cognitive impairment was related to CBF reduction in white matter but not to the extent of WMA in 57 patients with cerebral microangiopathy different from CADASIL. We recently reported, in vivo, that the severity of ultrastructural white matter changes was strongly related to the severity of clinical status in CADASIL.[9] Therefore, whether the degree of blood flow reduction in WMA is related to the severity of white matter rarefaction in CADASIL should be investigated specifically.

We did not find a significant decrease of absolute CBF or CBV values in the cortex of patients with CADASIL. These results are in contrast with the reduction of cortical CBF reported in the only comparable study performed with PET in 2 affected subjects with widespread WMA.[11] Previous data concerning cortical blood flow changes in other patients with "leukoaraiosis" appear to be controversial. In nondemented subjects, Turc et al[40] did not find any significant CBF or CBV modifications in the cortex, whereas other authors reported cortical CBF reduction related to the extent of WMA.[45–47] In demented patients, cortical CBF changes have been repeatedly reported in either a regional[38] or diffuse pattern.[37,42,48] The present negative findings might be related to the heterogeneity of our population, which included both demented and nondemented subjects. However, in contrast to the results

obtained in white matter, we did not find a relationship between cortical blood flow and dementia in our patients. It is noteworthy that only 1 of our patients presented with severe dementia. Nevertheless, these negative results might also be explained by the large variance in our absolute CBF and CBV measures at the cortical level, impeding the detection of moderate changes between samples of modest size. Therefore, further studies appear necessary to assess modifications of absolute CBF or CBV at the cortical level in CADASIL.

After the use of a normalization procedure to increase the regional contrasts,[49] we detected a significant reduction in relCBV and relCBF and increase in relMTT in the occipital cortex of our patients. These results differ from those of Mellies et al,[12] who reported a significant reduction in relative blood flow predominant in the frontal and temporal cortex in patients with CADASIL. This discrepancy might be related to the acquisition of only 7 planes with a gap of 5 mm between slices and the elimination of mediofrontal and temporal cortex in our study and to the exclusion of occipital regions in the analysis of Mellies et al.[12] Elsewhere, we did not find any significant regional difference in the cortex between demented and nondemented patients in the relative perfusion data, in agreement with the neuroimaging data previously obtained in demented patients with CADASIL that showed a mainly diffuse cortical CBF decrease.[11,12]

In the cortex of our patients, the ACZ effect on CBF and CBV did not differ from that observed in control subjects, which suggests a preserved hemodynamic reserve at the cortical level in CADASIL. In the white matter, the effect of ACZ remains highly significant, but the CBF increase in WMA in CADASIL was lower than that measured in the white matter of our control subjects. Interestingly, no significant change in MTT was detected in WMA, whereas a downward trend was present in the white matter of control subjects. Such data indicate a partial loss of ACZ vasoreactivity within areas of increased T2 signal in CADASIL. ACZ is presumed to decrease smooth muscle tone in the walls of small arteries and to reduce the resistance of the precapillary circulation, thereby increasing blood flow through the capillary bed with expansion and recruitment of perfused vessels.[50] The loss of smooth muscle cells and the severe ultrastructural changes observed at the arteriolar level in the white matter of patients with CADASIL[51] might explain the present results. Interestingly, after ACZ administration, the absolute CBF and CBV values in WMA remains lower than those measured after ACZ in the normal white matter. This difference cannot be explained only by the reduction in the absolute CBF increase. Consequently, the maximal vessel capacitance might also be reduced in the abnormal white matter of patients with CADASIL. A permanent reduction in the number of perfused vessels, a decrease in the maximal lumen of arterioles and capillaries, or both might explain these findings. In previous pathological reports, a reduction in the lumen of small perforating arteries has indeed been reported in this condition.[8,52] Furthermore, Ruchoux et al[10,51] described a loss in some white matter vessels of the major components of the wall replaced by fibrosis. These severe ultrastructural modifications probably induce changes in elasticity and capacitance of small vessels with important alterations of local hemodynamics. Elsewhere, the reduction of CBV in both the NAWM and WMA with the relative preservation of hemodynamic reserve in patients with CADASIL may also indicate that maximal vasodilation, as observed after the reduction in perfusion pressure at distance from a large artery occlusion,[41] was not present in the vascular network of our patients. This might be related to metabolic depression associated with white matter rarefaction but also to the possible disruption of the signal pathway underlying spontaneous compensatory vasodilation within the vascular wall.

The present results suggest that it is possible to increase cerebral perfusion with a pharmacological tool in CADASIL. The persistent effect of ACZ at the cortical level despite the loss of smooth muscle cells within arterioles might be related to the relaxation of larger arterial trunks, which are less affected in this disease.[10] Weller et al[53] reported that the frequency of migraine with aura, often observed in CADASIL, was dramatically reduced by ACZ in 1 patient with CADASIL. In the present study, we detected a significant decrease in relCBF and relCBV and increase in relMTT in the occipital cortex of patients with CADASIL, half of whom had a previous history of migrainous aura. The interpretation of these results should be cautious due to the already mentioned limitations of the methods to investigate blood flow at the cortical level and particularly within posterior areas.[14] However, it is noteworthy that a similar transient but more severe pattern of hemodynamic alterations has been reported during spontaneous migrainous aura in healthy subjects with the same technique.[54] Therefore, it is conceivable that cortical oligemia, as actually confirmed in only 1 asymptomatic patient,[11] might favor migrainous aura in some affected subjects and that this CBF decrease could be relieved with ACZ treatment. Other investigations are needed to confirm such an hypothesis. At the subcortical level, it is also necessary to determine whether the effect of ACZ may be helpful for the protection of white matter and basal ganglia despite the severe vascular changes observed at the capillary level.

Acknowledgments

References

1. Joutel A, Corpechot C, Ducros A, Vahedi K, Chabriat H, Mouton P, Alamowitch S, Domenga V, Cecillion M, Marechal E, Maciazek J, Vayssiere C, Cruaud C, Cabanis EA, Ruchoux MM, Weissenbach J, Bach JF, Bousser MG, Tournier-Lasserve E. Notch3 mutations in CADASIL, a hereditary adult-onset condition causing stroke and dementia. *Nature*. 1996;383:707–710.
2. Tournier-Lasserve E, Joutel A, Melki J, Weissenbach J, Lathrop GM, Chabriat H, Mas JL, Cabanis EA, Baudrimont M, Maciazek J, Bach MA, Bousser MG. Cerebral autosomal dominant arteriopathy with subcortical infarcts and leukoencephalopathy maps to chromosome 19q12. *Nat Genet*. 1993;3:256–259.

3. Chabriat H, Vahedi K, Iba-Zizen MT, Joutel A, Nibbio A, Nagy TG, Krebs MO, Julien J, Dubois B, Ducrocq X, Levasseur M, Homeyer M, Mas JL, Lyon-Caen O, Tournier-Lasserve E, Bousser MG. Clinical spectrum of CADASIL: a study of 7 families: cerebral autosomal dominant arteriopathy with subcortical infarcts and leukoencephalopathy. *Lancet*. 1995;346:934–939.

4. Chabriat H, Levy C, Taillia H, Iba-Zizen MT, Vahedi K, Joutel A, Tournier-Lasserve E, Bousser MG. Patterns of MRI lesions in CADASIL. *Neurology*. 1998;51:452–457.

5. Tournier-Lasserve E, Iba-Zizen MT, Romero N, Bousser MG. Autosomal dominant syndrome with stroke-like episodes and leukoencephalopathy. *Stroke*. 1991;22:1297–1302.

6. Dichgans M, Filipi M, Brüning R, Iannucci G, Berchtenbreiter C, Minicucci L, Uttner I, Crispin A, Ludwig H, Gasser T, Yousry T. Quantitative MRI in CADASIL. *Neurology*. 1999;52:1361–1367.

7. Skehan SJ, Hutchinson M, MacErlaine DP. Cerebral autosomal dominant arteriopathy with subcortical infarcts and leukoencephalopathy: MR findings. *Am. J. Neuroradiol*. 1995;16:2115–2119.

8. Baudrimont M, Dubas F, Joutel A, Tournier-Lasserve E, Bousser M. Autosomal dominant leukoencephalopathy and subcortical ischemic strokes: a clinicopathological study. *Stroke*. 1993;24:122–125.

9. Chabriat H, Pappata S, Poupon C, Clark C, Vahedi K, Poupon F, Mangin J, Pachot-Clouard M, Jobert A, Le Bihan D, Bousser M. Clinical severity in CADASIL related to ultrastructural damage in white matter: in vivo study with diffusion tensor MRI. *Stroke*. 1999;30:2637–2643.

10. Ruchoux MM, Maurage CA. CADASIL. Cerebral autosomal dominant arteriopathy with subcortical infarcts and leukoencephalopathy. *J Neuropathol Exp Neurol*. 1997;56:947–964.

11. Chabriat H, Bousser MG, Pappata S. Cerebral autosomal dominant arteriopathy with subcortical infarcts and leukoencephalopathy: a positron emission tomography study in two affected family members. *Stroke*. 1995;26:1729–1730.

12. Mellies JK, Baumer T, Muller JA, Tournier-Lasserve E, Chabriat H, Knobloch O, Hackeloer HJ, Goebel HH, Wetzig L, Haller P. SPECT study of a German CADASIL family: a phenotype with migraine and progressive dementia only. *Neurology*. 1998;50:1715–1721.

13. Ostergaard L, Weisskoff RM, Chesler DA, Gyldensted C, Rosen BR. High resolution measurement of cerebral blood flow using intravascular tracer bolus passages, part I: mathematical approach and statistical analysis. *Magn Reson Med*. 1996;36:715–725.

14. Ostergaard L, Sorensen AG, Kwong KK, Weisskoff RM, Gyldensted C, Rosen BR. High resolution measurement of cerebral blood flow using intravascular tracer bolus passages, part II: experimental comparison and preliminary results. *Magn Reson Med*. 1996;36:726–736.

15. Ostergaard L, Johannsen P, Host-Poulsen P, Vestergaard-Poulsen P, Asboe H, Gee AD, Hansen SB, Cold GE, Gjedde A, Gyldensted C. Cerebral blood flow measurements by magnetic resonance imaging bolus tracking: comparison with [^{15}O]H$_2$O positron emission tomography in humans. *J Cereb Blood Flow Metab*. 1998;18:935–940.

16. Ostergaard L, Smith DF, Vestergaard-Poulsen P, Hansen SB, Gee AD, Gjedde A, Gyldensted C. Absolute cerebral blood flow and blood volume measured by magnetic resonance imaging bolus tracking: comparison with positron emission tomography values. *J Cereb Blood Flow Metab*. 1998;18:425–432.

17. Joutel A, Vahedi K, Corpechot C, Troesch A, Chabriat H, Vayssiere C, Cruaud C, Maciazek J, Weissenbach J, Bousser MG, Bach JF, Tournier-Lasserve E. Strong clustering and stereotyped nature of Notch3 mutations in patients with CADASIL. *Lancet*. 1997;350:1511–1515.

18. Cockrell JR, Folstein MF. Mini-Mental State Examination (MMSE). *Psychopharmacol Bull*. 1988;24:689–692.

19. De Haan R, Limburg M, Bossuyt P, Van der Meulen J, Aaronson N. The clinical meaning of Rankin "handicap" grades after stroke. *Stroke*. 1995; 26:2027–2030.

20. *Diagnostic and Statistical Manual of Mental Disorders*, ed 3. Washington, DC: American Psychiatric Association; 1987.

21. Stables L, Kennan R, Gore J. Asymmetric spin-echo imaging of magnetically inhomogeneous systems: theory, experiment and numerical studies. *Magn Reson Med*. 1998;40:432–442.

22. Boxerman J, Hamberg L, Rosen B, Weiskoff R. MR contrast due to intravascular magnetic susceptibility perturbations. *Magn Reson Med*. 1995;34:555–566.

23. Dahl A, Russel D, Rootwelt D, Nyberg-Hansen R, Kerty E. Cerebral vasoreactivity assessed with transcranial Doppler and regional cerebral blood flow measurements: dose, serum concentration and time course of the response to acetazolamide. *Stroke*. 1995;26:2302–2306.

24. Villringer A, Rosen B, Belliveau J, Ackerman J, Lauffer R, Buxton R, Chao Y, Wedeen V, Brady T. Dynamic imaging with lanthanides chelates in normal brain: contrast due to magnetic susceptibility effects. *Magn Reson Med*. 1988;6:164–174.

25. Porkka L, Neuder M, Hunter G, Weiskoff R, Belliveau J, Rosen B. Arterial input function measurement with MRI. Proceedings of the 10th annual SMRM meeting, San Francisco, 1991, 120.

26. Leenders KL, Perani D, Lammertsma AA, Heather JD, Buckingham P, Healy MJ, Gibbs JM, Wise RJ, Hatazawa J, Herold S, Beaney RP, Brooks DJ, Spinks T, Rhodes C, Frackowiak RSJ, Jones T. Cerebral blood flow, blood volume and oxygen utilization: normal values and effect of age. *Brain*. 1990;113:27–47.

27. Van de Moortele PF, Cerf B, Lobel E, Paradis AL, Faurion A, Le Bihan D. Latencies in fMRI time-series: effect of slice acquisition order and perception. *NMR Biomed*. 1997;10:230–236.

28. Talairach P, Tournoux P. *Co-Planar Stereotaxic Atlas of the Human Brain: 3-Dimensional Proportional System: An Approach to Cerebral Imaging*. Stuttgart/New York: Thieme; 1988.

29. Guckel F, brix G, Schmiedek P, Piepgras A, Becker G, Köpke J, Gross H, Georgi M. Cerebrovascular reserve capacity in patients with occlusive cerebrovascular disease: assessment with dynamic susceptibility contrast-enhanced MR imaging and the acetazolamide stimulation test. *Radiology*. 1996;201:405–412.

30. Ojemann J, Akbudak E, Snyder A, McKinstry R, Raichle M, Conturo T. Anatomic localization and quantitative analysis of gradient refocused echo-planar fMRI susceptibility artifacts. *Neuroimaging*. 1997;6: 156–167.

31. Schreiber W, Gückel F, Stritzke P, Schmiedek P, Schwartz A, Brix G. Cerebral blood flow and cerebroreserve capacity: estimation by dynamic magnetic resonance imaging. *J Cereb Blood Flow Metab*. 1998;18: 1143–1156.

32. Rempp K, Brix G, Wenz F, Becker C, Gückel F, Lorenz W. Quantification of regional cerebral blood flow and volume with dynamic susceptibility contrast-enhanced MR Imaging. *Radiology*. 1994;193:637–641.

33. Petrella J, DeCarli C, Dagli M, Duyn J, Grandin C, Frank J, Hoffman E, Theodore W. Assessment of whole-brain vasodilatory capacity with acetazolamide challenge at 1.5 T using dynamic contrast imaging with frequency-shifted burst. *Am J Neuroradiol*. 1997;18:1153–1161.

34. Démolis P, Tran Dinh Y, Giudicelli J. Relationships between cerebral regional blood flow velocities and volumetric blood flows and their respective reactivities to acetazolamide. *Stroke*. 1996;27:1835–1839.

35. Kiss B, Dallinger S, Findl O, Rainer G, Eichler H, Schmetterer L. Acetazolamide-induced cerebral and ocular vasodilation in humans is independent of nitric oxide. *Am J Physiol*. 1999;276:R1661–R1667.

36. Bickler P, Litt L, Severinghaus J. Effects of acetazolamide on cerebrocortical NADH and blood volume. *J Appl Physiol*. 1988;65:428–433.

37. Yao H, Sadoshima S, Ibayashi S, Kuwabara Y, Ichiya Y, Fujishima M. Leukoaraiosis and dementia in hypertensive patients. *Stroke*. 1992;23: 1673–1677.

38. De Reuck J, Decoo D, Strijckmans K, Lemahieu I. Does the severity of leukoaraiosis contribute to senile dementia? A comparative computerized and positron emission tomographic study. *Eur Neurol*. 1992;32:199–205.

39. Oishi M, Mochizuki Y, Takasu T. Blood flow differences between leukoaraiosis with and without lacunar infarction. *Can J Neurol Sci*. 1998;25: 70–75.

40. Turc J, Chollet F, Berry I, Sabatini U, Démonet J, Celsis P, Marc-Vergnes J, Rascol A. Cerebral blood flow, cerebral blood flow reactivity to acetazolamide, and cerebral blood volume in patients with leukoaraïosis. *Cerebrovasc Dis*. 1994;4:287–293.

41. Yamaguchi H, Fukuyama H, Harada K, Yamaguchi S, Miyoshi T, Doi T, Kimura J, Iwasaki Y, Asato R, Yonekura Y. White matter hyperintensities may correspond to areas of increased blood volume: correlative MR and PET observations. *J Comput Assist Tomogr*. 1990;14:905–908.

42. Kuwabara Y, Ichiya Y, Sasaki M, Yoshida T, Fukumura T, Masuda K, Ibayashi S, Fujishima M. Cerebral blood flow and vascular response to hypercapnia in hypertensive patients with leukoaraiosis. *Ann Nucl Med*. 1996;10:293–298.

43. De Reuck J, Van Acken J, Decoo D, Strijckmans K, Lemahieu I. Cerebral blood flow and oxygen metabolism in leukoaraïosis. A positron emission tomography study. *Cerebrovasc Dis*. 1991;1:25–30.

44. Sabri O, Ringelstein E, Hellwig D, Schneider R, Schreckenberger M, Kaiser H, Mull M, Buell U. Neuropsychological impairment correlates with hypoperfusion and hypometabolism but not with severity of white matter lesions on MRI in patients with cerebral microangiopathy. *Stroke*. 1999;30:556–566.

45. Kobari M, Meyer JS, Ichijo M, Oravez WT. Leukoaraiosis: correlation of MR and CT findings with blood flow, atrophy, and cognition. *AJNR Am J Neuroradiol*. 1990;11:273–281.

46. Isaka Y, Okamoto M, Ashida K, Imaizumi M. Decreased cerebrovascular dilatory capacity in subjects with asymptomatic periventricular hyperintensities. *Stroke*. 1994;25:375–381.

47. Meguro K, Hatazawa J, Yamaguchi T, Itoh M, Matsuzawa T, Ono S, Miyazawa H, Hishinuma T, Yanai K, Sekita Y, Yamada K. Cerebral circulation and oxygen metabolism associated with subclinical periventricular hyperintensity as shown by magnetic resonance imaging. *Ann Neurol*. 1990;28:378–383.

48. Kawamura J, Meyer JS, Terayama Y, Weathers S. Leukoaraiosis correlates with cerebral hypoperfusion in vascular dementia. *Stroke*. 1991;22:609–614.

49. Arndt S, Cizadlo T, O'Leary D, Gold S, Andreasen N. Normalizing counts and cerebral blood flow intensity in functional imaging studies of the human brain. *Neuroimage*. 1996;3:175–184.

50. Frankel H, Garcia E, Malik F, Weiss J, Weiss H. Effect of acetazolamide on cerebral blood flow and capillary patency. *J Appl Physiol*. 1992;73:1756–1761.

51. Ruchoux MM, Guerouaou D, Vandenhaute B, Pruvo JP, Vermersch P, Leys D. Systemic vascular smooth muscle cell impairment in cerebral autosomal dominant arteriopathy with subcortical infarcts and leukoencephalopathy. *Acta Neuropathol*. 1995;89:500–512.

52. Zhang W, Chun Ma K, Andersen O, Sourander P, Tolleson P, Olsson Y. The microvascular changes in cases of hereditary multi-infarct disease of the brain. *Acta Neuropathol*. 1994;87:317–324.

53. Weller M, Dichgans J, Klockgether T. Acetazolamide-responsive migraine in CADASIL. *Neurology*. 1998;50:1505.

54. Cutrer FM, Sorensen AG, Weisskoff RM, Ostergaard L, Sanchez del Rio M, Lee EJ, Rosen BR, Moskowitz MA. Perfusion-weighted imaging defects during spontaneous migrainous aura. *Ann Neurol*. 1998;43:25–31.